DOI 10.31489/2020Ph2/83-92

UDC 539.25

B.K. Rakhadilov[1], W.Wieleba[2], M.K. Kylyshkanov[1], A.B. Kenesbekov[1], M. Maulet[1]

[1]S. Amanzholov East Kazakhstan State University, Ust-Kamenogorsk, Kazakhstan;
[2]Wroclaw University of Science and Technology, Kazakhstan
(E-mail: rakhadilovb@mail.ru)

Structure and phase composition of high-speed steels

This work is devoted to the study of the structure and phase composition of high-speed steels R6M5, R9 and R18. High service properties of high-speed steel tools are achieved by heat treatment. Therefore, the sample blanks for the study were cut from cutting tools from R6M5, R9 and R18steels, which were subjected to the usual standard heat treatment for these steels. Installed that the structure of high-speed steels R6M5, R9 and R18 in the initial state, i.e. after standard heat treatment, consists of martensite and special carbides. The carbide particles are evenly distributed in the matrix and are close to the correct spherical shape. Thus in the structure of steels R6M5 and R9 are carbides of type M_6C, MC, and in the structure of steel R18 only carbides of the type M6C. EBSD analysis showed that M_6C carbides are most optimally combined with the Fe_3W_3C cubic phase, and the MS type carbide corresponds to the VC phase. Electron microscopic analysis showed that in addition to M_6C and MC carbides, high-speed steel contains small amounts of «cementite» type M_3C carbides.

Keywords: high-speed steel, structure, phase composition, carbide, heat treatment, cementite, martensite, tungsten.

Introduction

High cutting properties of high-speed steels are achieved by special alloying and complex heat treatment, providing a certain phase composition [1]. In addition, with cutting speed increases, the requirements for the heat resistance of steel increase [2]. The heat resistance of high-speed steels is due to alloying with their carbide-forming elements: tungsten, vanadium, molybdenum and chromium [3]. These elements, in certain temperature and time conditions, form in the steel particles of the carbide phase, which are the strengthening phase of the material [4,5]. A high heat resistance tool made of high-speed steels acquires after quenching and repeated tempering [6]. Tempering after quenching within the temperatures set for cutting tools leads to a decrease in the carbon content of martensite and the formation of ultramicroscopic carbides [7,8]. These carbides play an important role in the mechanical properties of steel, including in hardness, wear resistance, and heat resistance [9, 10]. Technological characteristics of high-speed steels are directly determined by the features of its microstructure. Therefore, research of the phase composition and fine structure of steel is a important objective. The main research methods previously used [11–13] were optical microscopy at small magnifications (up to 500 fold) and x-ray diffraction analysis. Quite often the main way to revelation and diagnostics the carbide phase was chemical dissolution and subsequent investigation of the sediment by x-ray diffraction analysis.

In this regard, the purpose of this work is to study and compare the structure and phase composition of high-speed steels R6M5, R9 and R18 using modern methods for studying the structure of metals and alloys.

Materials and methods of research

In accordance with the set tasks, tool high-speed steels R6M5, R9 and R18 were selected as the research material. The use of high-speed steels for cutting tools can increase the cutting speed several times, and the tool resistance-ten times [14]. The main distinguishing feature of high-speed steels is their high heat resistance or hardness (600–700^{o}C) in the presence of high hardness (63–70 HRC) and tool wear resistance. The unique properties of high-speed steels are achieved by special alloying and complex heat treatment, providing a certain phase composition [14]. Table 1 shows the chemical composition of high-speed steels R6M5, R9 and R18.

The choice of research materials is also justified by the fact that high-speed steels R6M5, R9, R18 are the most common in Metalworking, typical high-speed steels of moderate heat resistance [14].

Table 1

Chemical composition of high-speed steels R6M5, R9 and R18 (GOST 19265–73)

Steel grade	C	Mn	Si	Cr	W	V	Co	Mo	Ni	Cu	S	P
R9	0.85-0.95	before 0.50	before 0.50	3.80-4.40	8.50–9.50	2.30-2.70	before 0.50	before 1.00	before 0.40	-	before 0.03	before 0.03
R6M5	0.82-0.9	0,20-0.50	0,20-0.50	3.80-4.40	5.50-6.50	1.70–2.10	before 0.50	4.80–5.30	before 0.60	before 0.25	before 0.025	before 0.03
R18	0.73-0.83	0,20-0.50	0,20-0.50	3.80-4.40	17.00-18.50	1.00-1.40	before 0.50	before 1.00	before 0.60	before 0.25	before 0.03	before 0.03

High service properties of high-speed steel tools are achieved by heat treatment. Therefore, sample blanks with dimensions of 10x20x20 mm^3 for research were cut from cutting tools (disk cutter) made of R6M5, R9, and R18 steels subjected to the usual heat treatment for these steels [15] (Table 2).

Table 2

Modes of pre-heat treatment of high-speed steels

Steel grade	Types of heat treatment	
	Hardening	Tempering
R9	with 1240 °C in oil	560 °C (triple: the duration of each tempering is 1 h, cooling in the air)
R6M5	with 1230 °C in oil	560 °C (triple: the duration of each tempering is 1 h, cooling in the air)
R18	with 1270 °C in oil	560 °C (triple: the duration of each tempering is 1 h, cooling in the air)

Optical metallography was used to reveals the structure of the materials under study. An optical light microscope «ALTAMI-MET-1M» was used for metallographic analysis. For etching, a 4 % alcohol solution of nitric acid was used. X-ray diffraction studies samples of steel were performed using known methods of x-ray diffraction analysis using the D8 ADVANCE diffractometer. Diffractograms were taken using CuK_{α}-radiation (λ=2,2897 A˚) at a voltage of kV. Decrypting of diffractograms was carried out manually using standard techniques and the PDF-4 database, and the quantitative analysis was performed using the Powder Cell program. The morphology and elemental composition of the samples were studied a raster electron microscope JSM-6390LV. Studies of the phase composition of carbide phases and their sizes were performed EBSD analysis (diffraction analysis of backscattered electrons) on a system with electronic and focused ion beams Quanta 200 3D. Before the study, the samples were sanded and polished. For revealing the boundaries of the grains and particles of the carbide phases, chemical etching of the grinds in a 4 % alcohol solution of nitric acid was used (the etching time is 5–7 s). The structure and phase composition of R6M5 steel samples were investigated by the method transmission electron microscopy on thin foils with the help an EM-125 electron microscope at an accelerating voltage of 125 kV. Working magnification in the column of the microscope was chosen to be from 25000 to 50000 times To conduct research from the surface of the sample the sample was cut into plates (foil) with a thickness of 0.2–0.3 mm using electric spark cutting samples. The resulting foil was first thinned chemically in an electrolyte of 90 % hydrofluoric acid and 10 % perhydrol, and then electrolytically in a supersaturated solution of orthophosphoric acid with chromium anhydride at room temperature, an operating voltage of 20 V and a current density of 2–4 A/cm^2. The phase type was determined using images confirmed by microdiffraction patterns and dark-field images obtained in the reflexes of the corresponding phases.

Research results and Discussion

Figure 1 shows the microstructures of R6M5, R9 and R18 steels in their initial state, i.e. after standard heat treatment. The figure shows that the microstructures of R6M5, R9 and R18 steels are very similar to each other and consist of martensite tempering and special carbides (Figure 1).

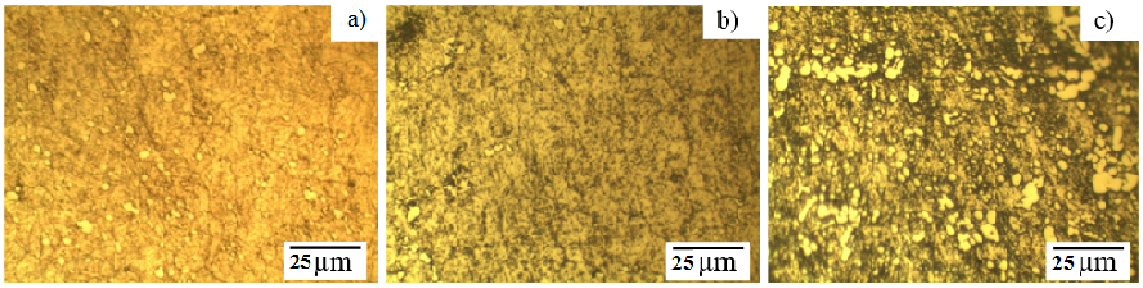

Figure 1. Microstructure of R6M5 (a), R9 (b) and R18 (c) steels

Figure 2 shows the SEM images of the surface of the steel R6M5, R9 and R18. The structure steel consists of martensite and carbides. The carbide particles are evenly distributed in the matrix and are close to the correct spherical shape. Two types of carbides are observed in the structure of high-speed steels R6M5 and R9: light and gray carbides (Figure 2 a, b, d). And only bright carbides are present in the structure of R18 steel (Figure 2c). Figure 2g shows the microstructure of R6M5 steel obtained using a semiconductor detector with backscattered electrons, giving surface pictures with chemical contrast with high spatial resolution. Grey carbides are clearly visible from this image. Thus, it can be established that after standard heat treatment, two types of carbides are present in the structure of R6M5 and R9 steels: very bright colors of carbides (bright carbides) are containing elements above the atomic number and gray carbides containing elements below the atomic number, and only bright carbides are present in the structure of R18 steel. The volume fraction of each fraction was evaluated. The sizes of carbide particles in the studied steels are also determined. The results of quantitative parameters of the steel structure are shown in Table 3.

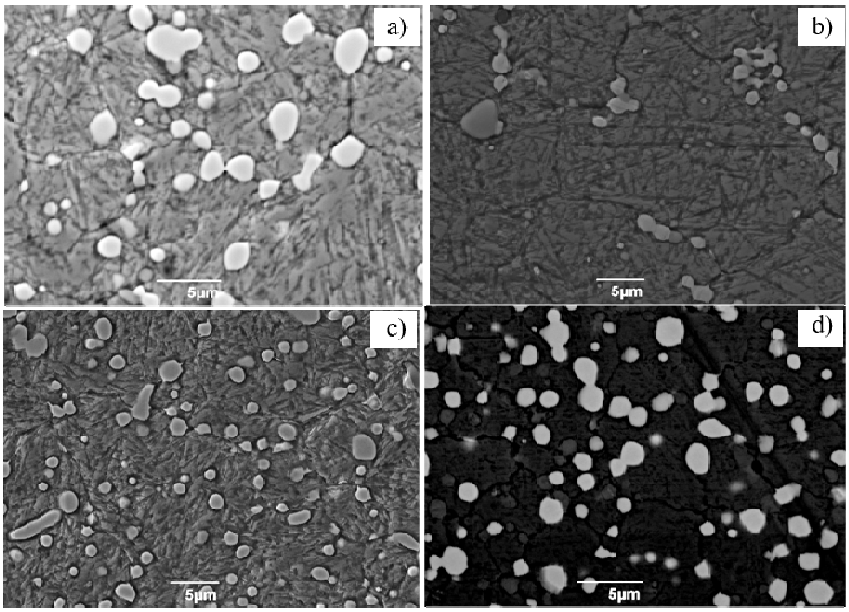

Figure 2. Microstructure of the surface of high-speed steels R6M5 (a, d), R9 (b), R18 (c)

Table 3

Quantitative parameters of structure of steel R6M5, R9 and R18

No	Sample	Carbides	Volume fraction	Average particle size
1	R6M5	bright carbides	10.4±0.6 %	2.1 µm
		dark carbides	2.3±0.4 %	0.8 µm
2	R9	bright carbides	3.1±0.6 %	1.6 µm
		dark carbides	1.7±0.4 %	1.8 µm
3	R18	bright carbides	13.4±0.6 %	1.9 µm

To identify the composition of carbides and their distribution, a map of the distribution of alloying elements in the steel structure was obtained. The General distribution of alloying elements in the structure of R6M5, R9, and R18 steels is shown in Figures 3, 4, and 5, respectively. The drawings show that the bright spherical carbides are enriched with tungsten and molybdenum, while the gray ones are enriched with vanadium. The obtained maps of the distribution of alloying elements confirmed that there present two types of carbides in the structure of R6M5 and R9 steels — bright and dark and only bright ones in the structure of R18 steel. The absence of gray carbides that are enriched with vanadium in the structure of R18 steel may be due to the fact that the content of vanadium in the composition of R18 steel is low compared to R6M5 and R9 steels. In addition, Figure 5 shows that the main mass of vanadium is located in bright carbides in the structure of R18 steel. It should be borne in mind that V, W, Mo, and Cr are carbide-forming elements. In other words, carbides of these metals have high binding energy and stability [15,16]. This is why most of the alloying elements are found in carbides, rather than in solid solution.

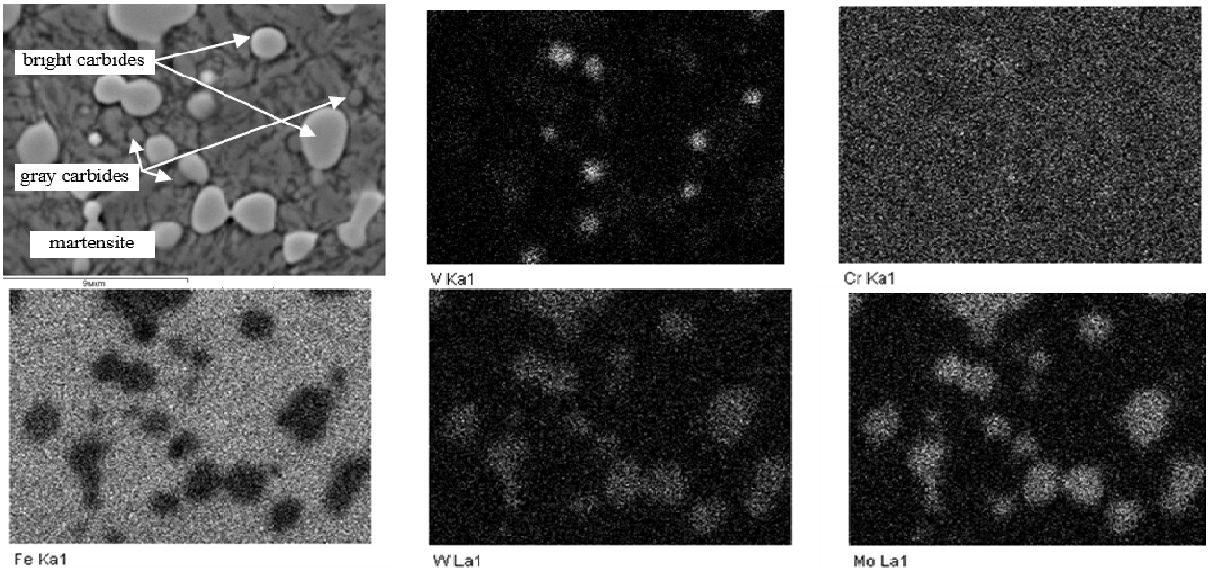

Figure 3. Surface microstructure and map distribution of R6M5 steel alloying elements

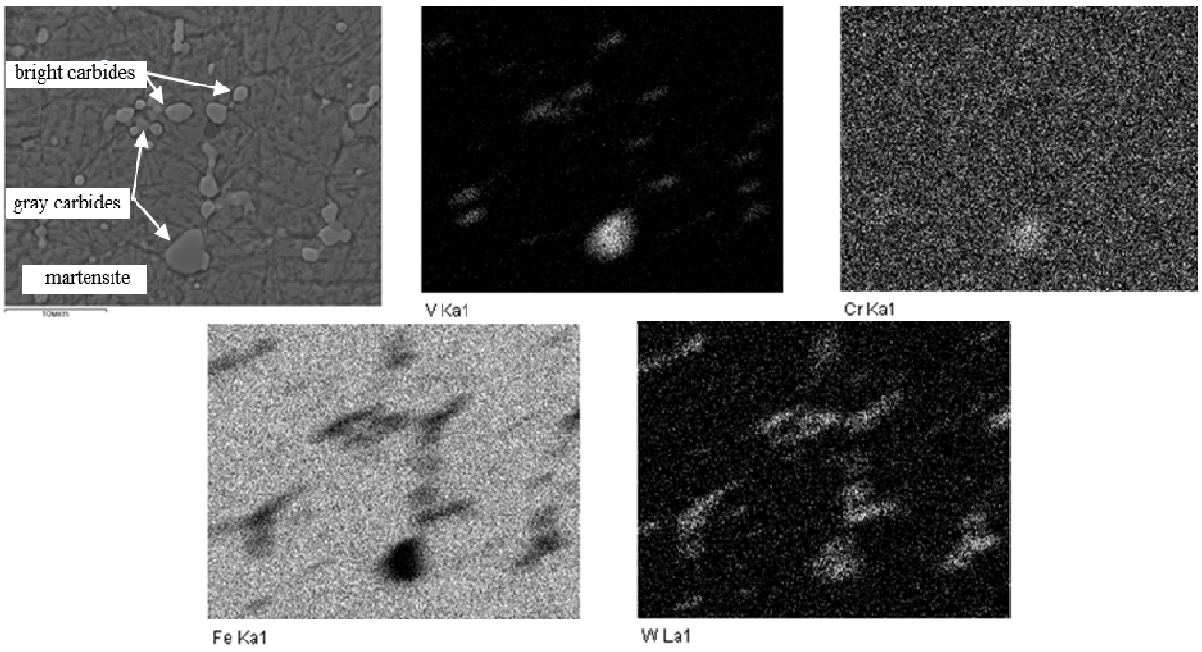

Figure 4. Surface microstructure and distribution map distribution of R9 steel alloying elements

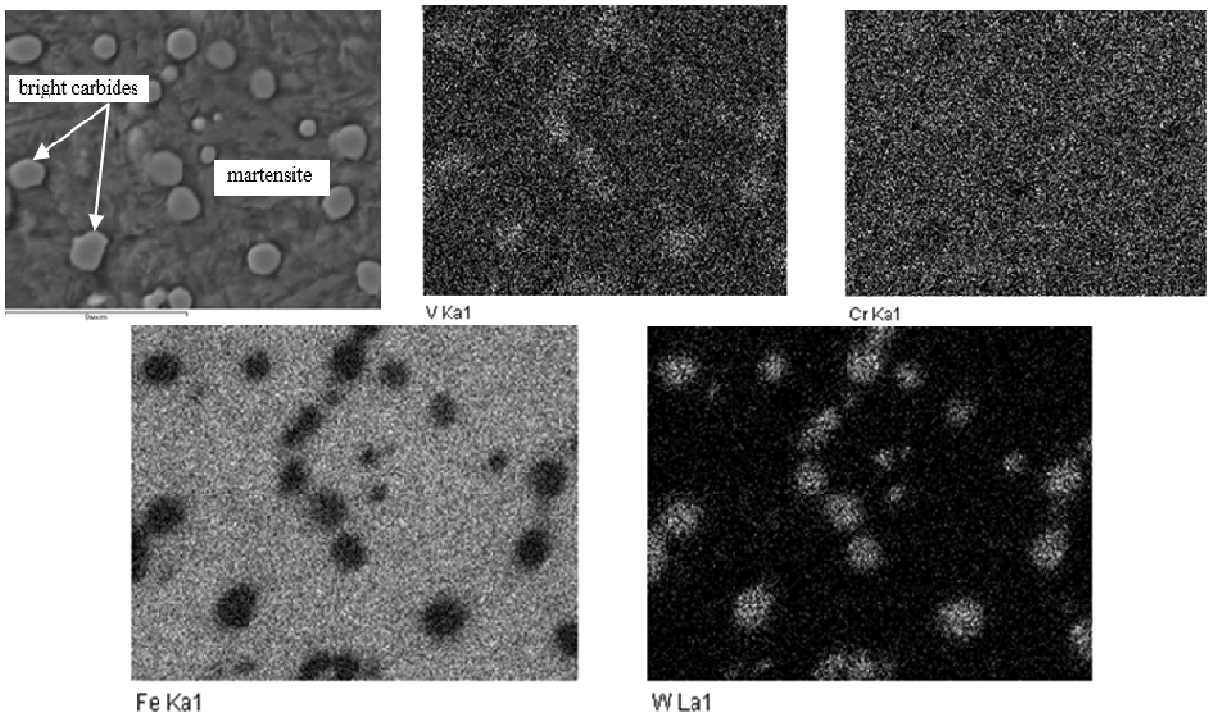

Figure 5. Surface microstructure and map distribution of R18 steel alloying elements

To determine the elemental composition of the particles of the released carbides and matrix (martensite), a microprobe analysis was performed (Figure 6). Table 4 shows the content of alloying elements in carbides and matrix for R6M5, R9 and R18 steels. Tungsten, molybdenum, vanadium, and chromium form special carbides in steel: M_6C based on tungsten and molybdenum, MC based on vanadium, and $M_{23}C_6$ based on chromium. The results of mapping and microprobe analysis show that M_6C and MC carbides are present in the structure of R6M5 steel after standard heat treatment, and $M_{23}C_6$ carbides are absent, which is in good agreement with the literature data [16–18]. However, in some papers [19,20], it is stated that after standard heat treatment, only M_6C-type carbide particles are present in the structure of R6M5 steel. Apparently, this is due to the small volume fraction of MC-type carbide particles and the similarity of these particles to the matrix, which does not allow them to be detected. In addition, the methods used in these studies have limitations when detecting carbide particles with a small concentration. Therefore, in this work, along with X-ray phase analysis, special methods of raster electron microscopy are used.

Table 4

Content of alloying elements in the structural constituent of high-speed steels

structural constituent	Content of elements, % (mass.)				
	V	Cr	Fe	Mo	W
R6M5					
Bright carbides	3.42	3.31	30.85	26.05	36.37
Dark carbides	26.47	4.45	30.82	16.62	21.64
Martensite	1.33	4.62	84.50	4.25	5.30
R9					
Bright carbides	3.15	3.52	28.83	3.1	61.4
Dark carbides	28.64	4.55	40.99	-	25.82
Martensite	3.11	4.95	80.78	-	11.16
R18					
Bright carbides	3.50	3.80	34.77	2.7	55.23
Martensite	1.07	4.64	84.39	-	9.90

The assumed configuration of M6C carbide is between the formulas $Fe_3(W, Mo)_3C$ — $Fe_3(W, Mo)_2C$ [21]. In other words, along with tungsten and molybdenum atoms, M6C carbide can located to 2/3 of the total number of metal atoms. Besides it, chromium and vanadium atoms can be dissolved, which replace iron atoms. Based on the results of the microprobe analysis, it can be assumed that the gray carbide particles are MC carbides based on vanadium.

Figure 6 shows diffractograms of R6M5, R9, and R18 steels. X-ray diffraction analysis showed that in the initial state, i.e., after heat treatment, the structure of R6M5 and R9 steels present the α-phase and M_6C, MC carbides, and only M_6C carbides in the structure of R18 steel. The results of X-ray diffraction analysis are shown in Table 5. Thus, X-ray diffraction analysis confirmed that the main carbides in the studied steel are M_6C and MC carbides. It was determined that M_6C type carbides that have a complex HCC crystal lattice and a spatial group Fd3m correspond to the composition of Fe_3W_3C, and MS type carbides that have a cubic crystal lattice and a spatial group Fm3m correspond to the composition of VC. It should be borne in mind that the M_6C type carbide can have the form of both Fe_3W_3C and Fe_3Mo_3C. As you know, one of the advantages of x-ray diffraction analysis (XRD) is that the peak position and lattice parameters can be determined fairly accurately. Nevertheless, in this case, when studying individual carbides, it is advisable to apply EBSD analysis. Therefore, to confirm the results of X-ray diffraction analysis was studied the crystal structure of M6C and MS carbides by EBSD analysis with help a reflected electron detector on a scanning microscope (system) with electronic and focused ion beams.

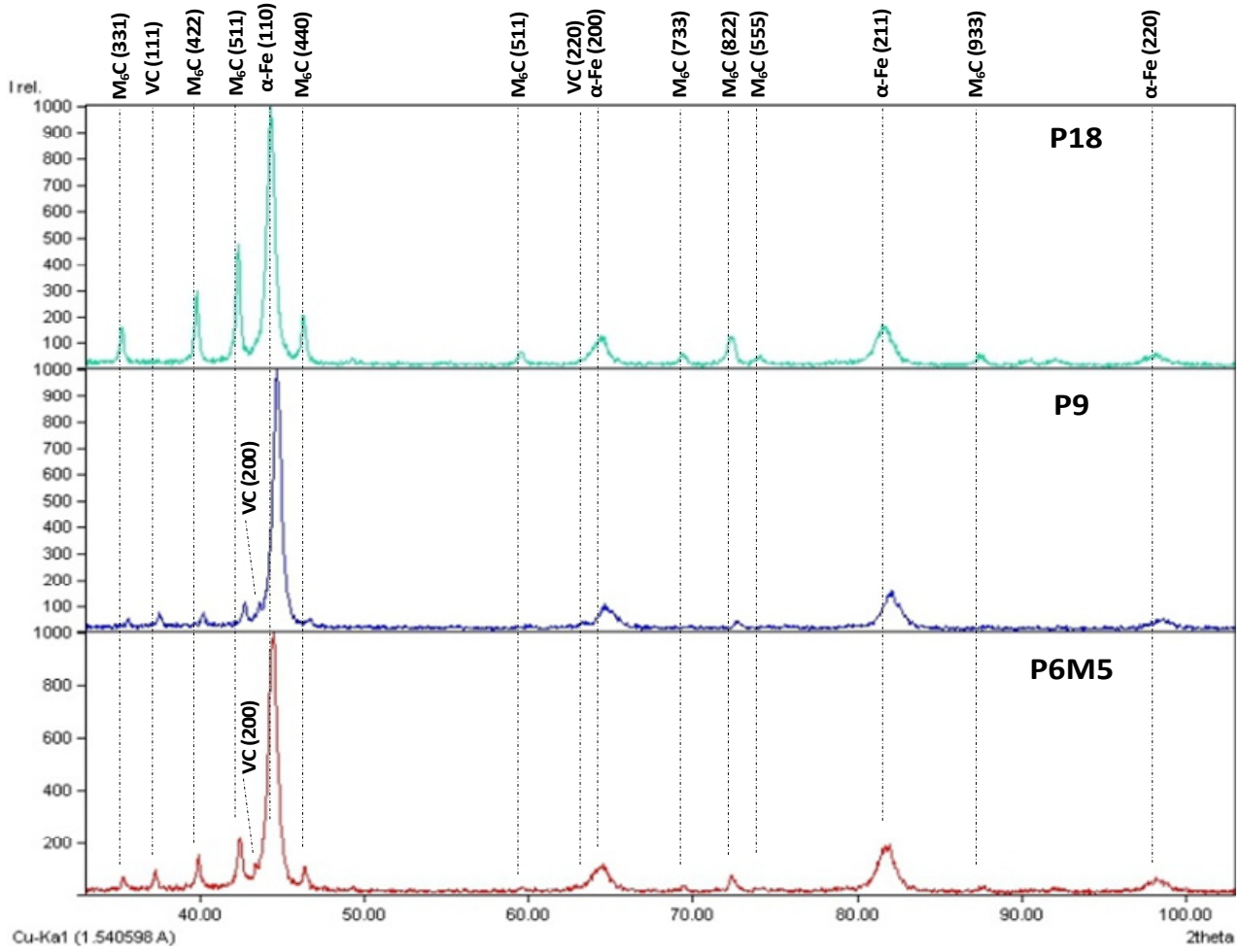

Figure 6. Diffractograms of high-speed steels in the initial state (after heat treatment)

Table 5

Results of x-ray diffraction analysis

Sample	The detected phase	Vol.frac.phases %	Lattice parameters, nm	The Sizes RCS, nm
R9, initial	α-Fe	81	0.28680	23.30 (all ref.)
	M_6C	11.8	1.10543	26.14 (100)
	MC	7.2	0.41566	25.01 (100)
R6M5, initial	α-Fe	75.2	0.28781	19.20 (all ref.)
	M_6C	13.7	1,10867	38.77 (all ref.)
	MC	11,1	0.41663	18.72 (100)
R18, initial	α-Fe	72.2	0.28720	50.36 (all ref.)
	M_6C	27.8	1.10429	39.43 (100)

Figure 7 shows the results of EBSD analysis of the R6M5 steel surface. EBSD analysis showed that tungsten-rich M_6C carbides are most optimally combined with the cubic phase of Fe_3W_3C, and MC-type carbides correspond to the VC phase. However, it is worth noting that in this case, Fe_3W_3C may also mean that other carbide-forming elements are present in the form of M_6C carbides.

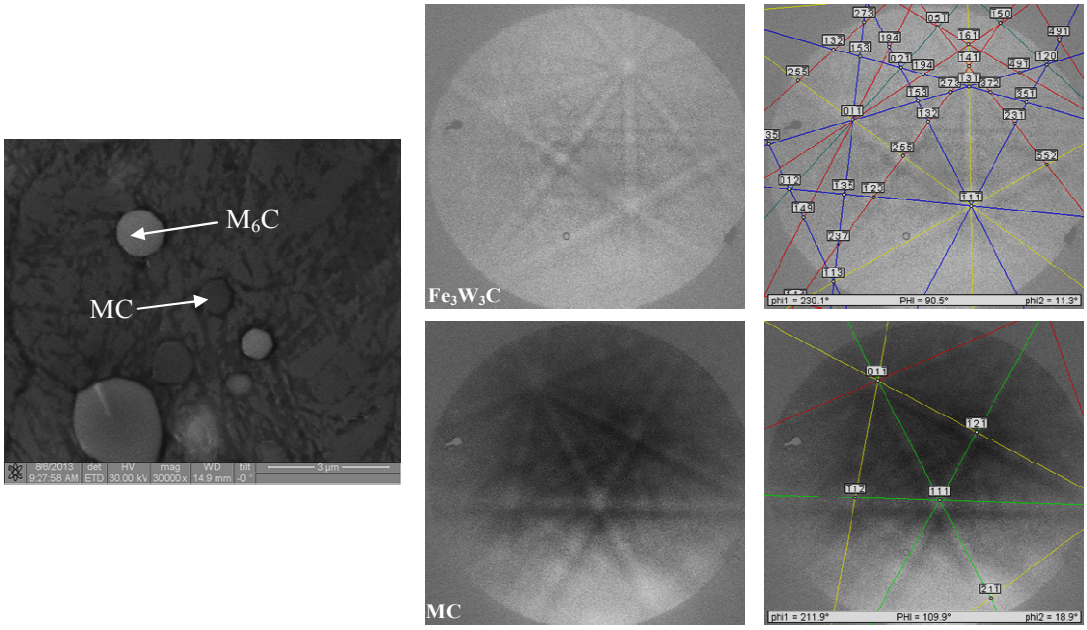

Figure 7. Results of EBSD analysis of R6M5 steel

Electron microscopic analysis showed that except in addition to M_6C and MC carbides, are present in steel in small amounts of carbides «cementite» type M_3C (Figure 8). Note the highest solubility in the cementite crystal lattice have that manganese and chromium atoms, slight solubility of the atoms of vanadium, molybdenum and tungsten. These particles are formed during quenching in the process of «self-leave» of steel due to the heat preserved in the material.

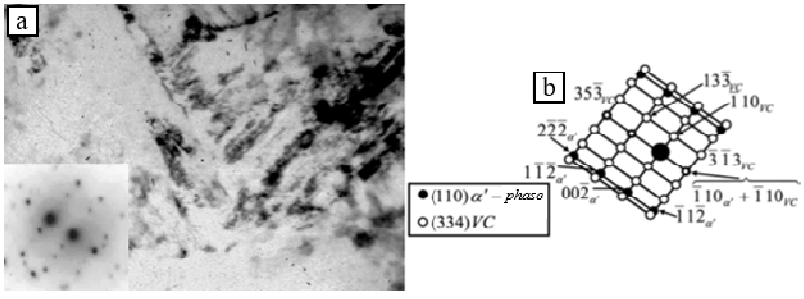

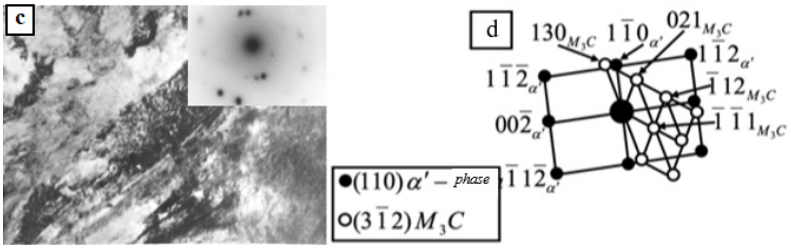

Figure 8. TEM image of P6M5 steel: a, c- brightfield image; b, d -induced microdiffraction pattern scheme

Thus, we characterized the structures and carbide phases of high-speed steels R6M5, R9 and R18 in the initial state, i.e. after standard heat treatment. The research of structural-phase states before a certain treatment is necessary in terms of revelation patterns of changes in the structure and its influence on properties. Since the physical and mechanical properties of high-speed steel in large measure by the structure and state of the carbide phases and their shape, size, and distribution in volume.

Conclusions

It was found that the structure of high-speed steels R6M5, R9 and R18 in the initial state, i.e. after standard heat treatment, consists of the α' — phase and special carbides. At that the structure of R6M5 and R9 steels contains M_6C and MC carbides, while in the structure of R18 steel contains only M_6C carbides type. Using method X-ray diffraction analysis and EBSD analysis, it was found that M_6C-type carbides which have a complex HCC crystal lattice and a spatial group Fd3m correspond to the composition of Fe_3W_3C, and MC-type carbides that have a cubic crystal lattice and a spatial group Fm3m correspond to the composition of VC.

This research is funded by the Science Committee of the Ministry of Education and Science of the Republic of Kazakhstan (Grant No. BR05236748).

References

1 Моисеев В.Ф. Инструментальные материалы / В.Ф. Моисеев, С.Н. Григорьев. — М.: МГТУ Станкин, 2005. — 248 с.

2 Firouzdor V. Effect of deep cryogenic treatment on wear resistance and tool life of M2 HSS drill / V. Firouzdor, E. Nejati, F. Khomamizadeh // Journal of Materials Processing Technology. — 2008. — Vol. 206(1–3). — P. 467–472.

3 Гученко С.А. Композиционные ионно-плазменные покрытия / С.А. Гученко, В.Ч. Лауринас, О.Н. Завацкая // Вестн. Караганд. ун-та. Сер. Физика. — 2014. — № 3(75). — С. 16–27.

4 Rahadilov B.K., Electrolyte-plasma surface hardening of 65G and 20GL low-alloy steels / B.K. Rakhadilov, L.G. Zhurerova, A.V. Pavlov, W. Wieleba // Bulletin of the University of Karaganda-Physics. — 2016. — Vol. 4(84). — P. 8–14.

5 Skakov M. Microstructure and tribological properties of electrolytic plasma nitrided high-speed steel / M. Skakov, B. Rakhadilov, M. Scheffler, E. Batyrbekov // Materials Testing. — 2015. — 57(4). — C. 360–364.

6 Chaus A.S. Structure and Properties of Cast Rapidly Cooled High-Speed Steel R6M5 / A.S. Chaus, F.I. Rudnitskii // Metal Science and Heat Treatment. — 2003. — Vol. 45. — P. 157–162.

7 Liu ZY. Microstructure evolution during sintering of injection molded M2 high speed steel / ZY. Liu, NH. Loh, KA. Khor, SB.Tor // Materials Science and Engineering A. — 2000. — Vol. 293(1–2). — P. 46–55.

8 Candane D. Effect of cryogenic treatment on microstructure and wear characteristics of AISI M35 HSS / D. Candane, N. Alagumurthi, K. Palaniradja // International Journal of Materials Science and Applications. — 2013. — Vol. 2(2). — P. 56–65.

9 Šolić S. Effect of deep cryogenic treatment on mechanical and tribological properties of PM S390 MC high-speed steel / S. Šolić, F. Cajner, V. Leskovšek // MP Materials Testing. — 2012. — Vol. 10. — P. 688–693.

10 Skakov M. Influence of electrolyte plasma treatment on structure, phase composition and microhardness of steel P6M5 / M. Skakov, B. Rakhadilov, M. Sheffler // Key Engineering Materials. — 2013. — Vol. 531–532. — P. 627–631.

11 Самсонов Г.В. Тугоплавкие соединения / Г.В. Самсонов, И.М. Винницкий. — М.: Металлургия, 1976. — 560 с.

12 Геллер Ю.А. Инструментальные стали / Ю.А. Геллер. — М.: Металлургия, 1983. — 527 с.

13 Bochnowskia W. Primary and secondary carbides in high-speed steels after conventional heat treatment and laser modification / W. Bochnowskia, H. Leitner, Ł. Majorc, R. Ebner, B. Major // Materials Chemistry and Physics. — 2003. — Vol. 81(2–3). — P. 503–506.

14 Гольдштейн М.И. Специальные стали / М.И. Гольдштейн, С.В. Грачев, Ю.Г. Векслер // Специальные стали. — М.: Металлургия, 1985. — 408 с.

15 Гуляев А.П. Теория быстрорежущей стали / А.П. Гуляев // МиТОМ. — 1998. — № 11. — С. 27–32.

16 Кремнев Л.С. Теория легирования и создание на ее основе теплостойких инструментальных сталей и сплавов оптимального состава / Л.С. Кремнев // Металловедение и термическая обработка металлов. — 2008. — № 11. — С. 18–28.

17 Skakov M. Specifics of microstructure and phase composition of high-speed steel R6M5 / M. Skakov, B. Rakhadilov, G. Karipbayeva // Applied Mechanics and Materials. — 2013. — Vol. 404. — P. 20–24.

18 Воробьева Г.А. Инструментальные материалы: инструментальные стали и сплавы / Г.А. Воробьева, Е.Е. Складнова. — Ч. 1. — СПб., 2003. — 100 с.

19 Guenzel R. Pulsed electron-beam treatment of high-speed steel current tools: struchire-phase transformation and wear resistance / R. Guenzel, W. Matz, Yu.F. Ivanov, V.P. Rothtein // 1st International Congress on Radiation Physics, high current electronics, and modification of materials. — Tomsk, Russia. — 2000. — Vol. 3. — P. 303–307.

20 Ivanov Yu. Pulsed electron beams melting of high-speed steel: structural phase transformations and wear resistance / Yu. Ivanov, W. Matz, V. Rotshtein, R. Gunzel, N. Shevchenko // Surface and Coatings Technology. — 2002. — No. 150. — P. 188–198.

21 Гольдшмидт Х.Дж. Сплавы внедрения / Х.Дж. Гольдшмидт. — М.: Мир, 1971. — 424 с.

Б.К. Рахадилов, В. Виелеба, М.К. Кылышканов, А.Б. Кенесбеков, М. Маулет

Жылдамкесетін болаттардың құрылымы мен фазалық құрамы

Мақала Р6М5, Р9 және Р18 жылдамкесетін болаттардың құрылымы мен фазалық құрамын зерттеуге арналған. Жылдамкескіш болаттан жасалған құралдың жоғары қызметтік қасиеттеріне термиялық өңдеу арқылы қол жеткізіледі. Сондықтан зерттеуге арналған үлгі дайындамалары Р6М5, Р9 және Р18 болаттарынан жасалған кескіш құралдардан, осы болаттар үшін стандартты термоөңдеуге ұшыраған. Бастапқы күйіндегі Р6М5, Р9 және Р18 жылдамкесетін болаттардың құрылымы, яғни стандартты термоөңдеуден кейін мартенсит пен арнайы карбидтерден тұрады. Карбидтердің бөлшектері матрицада біркелкі бөлінген және дұрыс сфералық формаға жақын. Бұл ретте Р6М5 және Р9 болаттарының құрылымында M_6C, МС типті карбидтер, ал Р18 болатының құрылымында тек M_6C типті карбидтер бар. КШЭД (EBSD)-талдау M_6C карбидтері Fe_3W_3C кубтық фазасымен ең оңтайлы үйлесетінін көрсеткен, ал МС типті карбид VC фазасына сәйкес келеді. Электрондық-микроскопиялық талдау тез кесілетін болаттағы M_6C және МС карбидтерінен басқа M_3C «цементитті» типті карбидтердің аз мөлшерде бар екені анықталған.

Кілт сөздер: жылдамкесетін болат, құрылым, фазалық құрам, карбид, термиялық өңдеу, цементит, мартенсит, вольфрам.

Б.К. Рахадилов, В. Виелеба, М.К. Кылышканов, А.Б. Кенесбеков, М. Маулет

Структура и фазовый состав быстрорежущих сталей

Статья посвящена исследованию структуры и фазового состава быстрорежущих сталей Р6М5, Р9 и Р18. Высокие служебные свойства инструмента из быстрорежущей стали достигаются термической обработкой. Поэтому заготовки образцов для исследования вырезали из режущих инструментов из сталей Р6М5, Р9 и Р18, подвергнутых обычной для этих сталей стандартной термообработке. Установлено, что структура быстрорежущих сталей Р6М5, Р9 и Р18 в исходном состоянии, т.е. после стандартной термообработки, состоит из мартенсита и специальных карбидов. Частицы карбидов равномерно распределены в матрице и близки к правильной сферической форме. При этом в структуре сталей Р6М5 и Р9 присутствуют карбиды типа M_6C, МС, а в структуре стали Р18 — только карбиды типа M_6C. ДОРЭ (EBSD)-анализ показал, что карбиды M_6C наиболее оптимально сочетаются с кубической фазой Fe_3W_3C, а карбидам типа МС соответствует фаза VC. Электронно-микроскопический анализ показал, что, кроме карбидов M_6C и МС, в быстрорежущей стали присутствуют в небольших количествах карбиды «цементитного» типа M_3C.

Ключевые слова: быстрорежущая сталь, структура, фазовый состав, карбид, термическая обработка, цементит, мартенсит, вольфрам.

References

1 Moiseev, V.F., & Grigorev, C.N. (2005). *Instrumentalnye materialy [Tool materials]*. (2d ed.). Moscow: MHTU Stankin [in Russian].

2 Firouzdor, V., Nejati, E., & Khomamizadeh, F. (2008). Effect of deep cryogenic treatment on wear resistance and tool life of M2 HSS drill. *Journal of Materials Processing Technology, 206(1–3),* 467–472.

3 Guchenko, S.A., Laurinas, V.Ch., & Zavatskaya, O.N. (2014). Kompozitsionnye ionno-plazmennye pokrytiia [Composite ion-plasma coatings]. *Vestnik Karahandinskoho universiteta. Seriia Fizika — Bulletin of the University of Karaganda. Physics series, 3(75),* 16–27 [in Russian].

4 Rahadilov, B.K., Zhurerova, L.G., Pavlov, A.V., & Wieleba, W. (2016). Electrolyte-plasma surface hardening of 65G and 20GL low-alloy steels. *Bulletin of the University of Karaganda-Physics, 4(84),* 8–14.

5 Skakov, M., Rakhadilov, B., Scheffler, M., & Batyrbekov, E. (2015). Microstructure and tribological properties of electrolytic plasma nitrided high-speed steel. *Materials Testing, 57(4),* 360–364.

6 Chaus, A.S., & Rudnitskii F.I. (2003). Structure and Properties of Cast Rapidly Cooled High-Speed Steel R6M5. *Metal Science and Heat Treatment, 45,* 157–162.

7 Liu, Z.Y., Loh, N.H., Khor, K.A., & Tor S.B. (2000). Microstructure evolution during sintering of injection molded M2 high speed steel. *Materials Science and Engineering A, 293,* 46–55.

8 Candane1, D., Alagumurthi, N., & Palaniradja K. (2013). Effect of cryogenic treatment on microstructure and wear characteristics of AISI M35 HSS. *International Journal of Materials Science and Applications, 2(2),* 56–65.

9 Šolić, S., Cajner, F., Leskovšek, V. (2012). Effect of deep cryogenic treatment on mechanical and tribological properties of PM S390 MC high-speed steel. *MP Materials Testing, 10,* 688–693.

10 Skakov, M., Rakhadilov, B., & Sheffler, M., (2013). Influence of electrolyte plasma treatment on structure, phase composition and microhardness of steel P6M5. *Key Engineering Materials, 531–532,* 627–631.

11 Samsonov, G.V., & Vinnitskii, I.M. (1976). *Tuhoplavkie soedineniia [Refractory compounds]*. Moscow: Metallurhiia [in Russian].

12 Geller, Yu.A. (1983). *Instrumentalnye stali [Tool steels]*. Moscow: Metallurhiia [in Russian].

13 Bochnowskiac, W., Leitnerb, H., Majorcd, Ł., Ebnerb, R., & Major, B. (2003). Primary and secondary carbides in high-speed steels after conventional heat treatment and laser modification. *Materials Chemistry and Physics, 81(2–3),* 503–506.

14 Goldishtein, M.I., Grachev, S.V. & Veksler, Yu.G. (1985). *Spetsialnye stali [Special steels]*. Moscow: Metallurhia [in Russian].

15 Guliaev, A.P. (1998). Teoria bystrorezhushei stali [Theory of high speed steel]. *MiTOM, 11,* 27–32 [in Russian].

16 Kremnev, L.S. (2008). Teoria lehirovaniia i sozdanie na ee osnove teplostoikikh instrumentalnykh stalei i splavov optimalnoho sostava [The alloying theory And the creation on its basis of heat-resistant tool steels and alloys of optimal composition]. *Metallovedenie i termicheskaia obrabotka metallov, 11,* 18–28 [in Russian].

17 Skakov, M., Rakhadilov, B., & Karipbayeva, G. (2013). Specifics of microstructure and phase composition of high-speed steel R6M5. *Applied Mechanics and Materials, 404,* 20–24.

18 Vorobeva, G.A., & Skladnova, E.E. (2003). *Instrumentalnye materialy: instrumentalnye stali i splavy [Tool Materials: Tool Steels & Alloys]*. Saint Petersburg [in Russian].

19 Guenzel, R., Matz, W., Ivanov, Yu.F., & Rothtein V.P. (2000). Pulsed electron-beam treatment of high-speed steel current tools: struchire-phase transformation and wear resistance. *1st International Congress on Radiation Physics, high current electronics, and modification of materials, 3,* 303–307. Tomsk, Russia.

20 Ivanov, Yu., Matz, W., Rotshtein, V., Gunzel, R., & Shevchenko N. (2002). Pulsed electron beams melting of high-speed steel: structural phase transformations and wear resistance. *Surface and Coatings Technology, 150,* 188–198.

21 Goldshmidt, H.Dzh. (1971). *Splavy vnedreniia [Introduction alloys]*. Moscow: Mir [in Russian].